

Proteinase-activated receptor-1, CCL2 and CCL7 regulate acute neutrophilic lung inflammation.

Running title: PAR₁ and acute neutrophilic inflammation.

Paul F. Mercer^{*1}, Andrew E. Williams^{*1}, Christopher J. Scotton^{*}, Ricardo J. José^{*}, Michael Sulikowski^{*}, James D. Moffatt[†], Lynne A. Murray[‡], and Rachel C. Chambers^{*}.

^{*}Centre for Inflammation and Tissue Repair, University College London (UCL),
WC1E 6JF United Kingdom

[†]Division of Biomedical Sciences, St George's, University of London, SW17 0QT
United Kingdom

[‡]Department of Immunobiology, Centocor Research and Development, USA

¹ **These authors contributed equally to this manuscript.**

Correspondence should be addressed to R.C.C (r.chambers@ucl.ac.uk), phone number:
+44(0)20 76796978, Fax: +44(0)20 76796973

Keywords.

Inflammation, lung, neutrophil, chemokine, PAR₁

Abstract.

PAR₁ plays a central role in mediating the interplay between coagulation and inflammation, but its role in regulating acute neutrophilic inflammation is unknown. We report that antagonism of PAR₁ was highly effective at reducing acute neutrophil accumulation in a mouse model of LPS-induced lung inflammation. PAR₁ antagonism also reduced alveolar-capillary barrier disruption in these mice. This protection was associated with a reduction in the expression of the chemokines CCL2 and CCL7, but not the pro-inflammatory cytokines TNF and IL-6 or the classic neutrophil chemoattractants CXCL1 and CXCL2. Antibody neutralisation of CCL2 and CCL7 significantly reduced LPS-induced total leukocyte and neutrophil accumulation, recovered from the bronchoalveolar lavage fluid of challenged mice. Immunohistochemical analysis revealed CCL2 predominantly localised to alveolar macrophages and pulmonary epithelial cells, while CCL7 was restricted to the pulmonary epithelium. In keeping with these observations, the intranasal administration of rCCL2 and rCCL7 led to the accumulation of neutrophils within the lung airspaces of naïve mice in the absence of any underlying inflammation. Flow cytometry analysis further demonstrated an increase in Ly6G^{hi} neutrophils expressing the chemokine receptors CCR1 and CCR2 isolated from mouse lungs compared to circulating neutrophils. Conversely, the expression of CXCR2 decreased on neutrophils isolated from the lung compared to circulating neutrophils. Furthermore, this switch in chemokine receptor expression was accentuated following acute LPS-induced lung inflammation. Collectively, these findings reveal a novel role for PAR₁ and the chemokines CCL2 and CCL7 during the early events of acute neutrophilic inflammation.

Introduction

The early stage of acute inflammation is usually associated with an influx of neutrophils into the injured tissue. Although this rapid innate immune response provides immediate host protection against infectious microorganisms, excessive leukocyte accumulation can lead to over-exuberant inflammation and tissue damage (1). Understanding the factors that control the early accumulation of neutrophils is critical in the context of both host defence and for the control of immunopathology associated with lung diseases such as acute respiratory distress syndrome (ARDS).

The lung epithelium functions as a mucosal barrier that prevents the entry of noxious substances from the environment and performs the essential function of gaseous exchange. It is therefore vital that pulmonary epithelial integrity is maintained in order to sustain these essential physiological functions. If this barrier is compromised, a complex series of pathways are initiated, involving the interplay between inflammation and coagulation, which provides host defence against infection and promotes wound healing and the maintenance of the endothelial-epithelial barrier (2). This process is highly complex and involves many factors, including cytokines, chemokines, growth factors, cell adhesion molecules and coagulation proteins.

Many of the cellular effects of coagulation proteinases are mediated via activation of the proteinase activated receptors (PARs), which are a family of G protein-coupled receptors (GPCRs) comprised of four members (PAR₁₋₄). Evidence obtained from biochemical studies and from knockout mice suggests a key role for the major high-affinity thrombin receptor PAR₁ in mediating the complex interplay between coagulation and inflammation in response to lung injury (2-5). It is known that PAR₁ regulates vascular integrity to systemic

inflammation and modulates the release of pro-inflammatory cytokines (6). This may involve complex interactions between various proteinases such as thrombin and matrix metalloproteinases, as well as inflammatory mediators. Activation of PAR₁ on epithelial cells, monocytes/macrophages and vascular endothelial cells leads to the release of pro-inflammatory mediators, including the cytokines TNF, IL-1 β , IL-2 and IL-6 and the chemokines CXCL8 (IL-8) and CCL2 (MCP-1) (2), mediators that have been directly associated with neutrophil activation, migration and the pathogenesis of ARDS (7, 8). Indeed, the alveolar-capillary barrier disruption associated with lung injury has been attributed to the immediate influx of neutrophils into the airspaces (9).

Neutrophils are constantly trafficking through the pulmonary circulation and are rapidly recruited into the lung in response to multiple inflammatory mediators, of which the chemokine CXCL8 (IL-8), and the functional mouse homologues CXCL1 (KC) and CXCL2 (MIP-2 α), are considered the most potent chemoattractants for neutrophil extravasation across endothelial and epithelial surfaces (1). Elevated levels of CXCL8 have also been associated with several inflammatory diseases, including ARDS (10). However, the contribution of other chemokines to neutrophil recruitment to the lung is less clear, although several studies have recently implicated CCL2 in this process (11, 12). CCL2, and the related chemokine CCL7, are predominantly associated with the egress of monocytes out of the bone marrow in response to pro-inflammatory stimuli (13-15), and the recruitment of monocytes and macrophages into peripheral tissue during episodes of inflammation or infectious disease (16, 17). However, it is uncertain if these CC-chemokines contribute to the early migration of neutrophils, in response to direct lung injury, or whether the lung affords unconventional chemotactic properties on migrating neutrophils.

We now demonstrate that inhibiting PAR₁ using a selective PAR₁ antagonist dampens the accumulation of neutrophils into alveolar spaces and reduces alveolar leak following LPS-induced inflammation. Furthermore, antagonism of PAR₁ attenuated the expression of the CC chemokines, CCL2 and CCL7, rather than mediators classically associated with neutrophil migration. Importantly, neutrophil recruitment into inflamed lung airspaces was significantly decreased by antibody neutralization of CCL2 and CCL7, demonstrating that both these chemokines play a key role in the trafficking of neutrophils into the inflamed lung. Immunohistochemical analysis revealed that both CCL2 and CCL7 predominantly immunolocalised to the pulmonary epithelium, although CCL2 also localised to the endothelium and alveolar macrophages. The instillation of recombinant CCL2 or CCL7 further confirmed a role for these chemokines in the recruitment of neutrophils into the lung. Moreover, CCL7 had a preferential effect on neutrophil accumulation compared to CCL2. Indeed, neutrophils isolated from lung tissue were found to express the chemokine receptors CCR1, CCR2 and CCR3, while CCR1 and CCR2 expression was further enhanced during inflammation. Taken together, these findings have important implications for our understanding of the interaction between coagulation and CC-chemokines during acute neutrophilic inflammation.

Materials and Methods

Pulmonary inflammation model.

Experiments were conducted with local ethical approval in accordance with the Home Office, UK. Female BALB/c mice (6-8 weeks; Charles River, UK) were anaesthetised (5% isofluorane) and challenged with LPS in sterile saline (125 µg/kg, 50 µl i.n.; *Escherichia coli* 0127:B8; Sigma, UK). Three hours later, animals were euthanised (urethane i.p. 20 g/kg), and bronchoalveolar lavage performed (3 × 0.5 ml to a total of 1.5 ml, PBS). Total and differential cell counts were quantified following cytopsin. Alternatively, BAL fluid was isolated and whole lungs were removed and homogenized.

Treatment protocols

Mice were injected i.p with the specific PAR₁ antagonist (αS)-N-[(1S)-3-amino-1-[[[(phenylmethyl)amino]carbonyl]propyl]-α-[[[[[1-(2,6-dichlorophenyl)methyl]-3-(1-pyrrolidinylmethyl)-1H-indazol-6-yl]amino]carbonyl]amino]-3,4-difluorobenzene]propanamide RWJ-58259 (5 mg/kg, a kind gift from Claudia Derian, Johnson and Johnson Pharmaceutical Research & Development, USA) 30 min after LPS administration. This antagonist is highly specific for PAR₁ and does not interact with other PARs or GPCRs. Formulations were used as described previously (18, 19). The specificity, pharmacological characteristics and optimal dosing regimen have been previously described (19-21) and the biological properties of the compound recently reviewed (22). In other experiments, mice received 10 µg (i.n.) anti-CCL2 (R&D Systems), anti-CCL7 (Peprotech), anti-CXCL10 (R&D Systems) or anti-CX3CL1 (R&D Systems) specific neutralising antibodies at the same time as LPS i.n.. BAL fluid was analysed at 3 hours. Recombinant

rCCL2 or rCCL7 (both Peprtech) were administered to Balb/c mice (500 ng/mouse i.n) in sterile PBS. BAL fluid was analysed at 3 hours as described above.

LDA PCR analysis

Total RNA was extracted from pulverised frozen lung using TRIzol (see manufacturer's protocol (Invitrogen)), DNase treated using a DNA free kit (Ambion) and cDNA synthesised from 1 µg RNA/per sample using a Superscript kit (Invitrogen). Expression levels of known inflammatory mediators were analysed in cDNA using Taqman low density array PCR chips and normalised to 18s. Relative differences in expression were calculated using the $\Delta\Delta CT$ method.

MPO, chemokine and protease measurement

Lung tissue homogenates were prepared as described previously (23). Briefly, frozen lung powder was mixed with PBS (10% w/v) containing protease inhibitors (Complete Mini; Roche Diagnostics, UK). Samples were homogenized on ice (Eppendorf), centrifuged (16,000g, 4°C, 15 min) and MPO measured by ELISA (Hycult Biotechnology). Serum albumin levels were measured by ELISA (Bethyl Laboratories). Chemokine levels in supernatants were measured by Luminex. IFN- γ , CCL2, CCL7 and IL-8 were also measured by ELISA (Peprtech). Thrombin-anti-thrombin levels were measured by ELISA (EnzymeResearch). Activated protein C, matrix metalloproteinase-1, MMP-2 and ELA-2 were also measured by ELISA (Antibodies Online). Receptor for advanced glycation endproducts (RAGE) was measured by ELISA (Abcam).

Immunohistochemical detection of CCL2, CCL7 and PAR₁

Briefly, mouse lungs were inflated with 4% formaldehyde, dehydrated through a serial alcohol gradient and embedded in paraffin wax. Serial sections (4 µm) were dewaxed and antigens unmasked by microwaving sections with 10 mM sodium citrate buffer (pH 6.0). Endogenous peroxidase activity was blocked with 3% hydrogen peroxide and sections were blocked with 3% horse serum with 1% BSA in PBS for goat primary antibodies and with 3% goat serum with 1% BSA in PBS for rabbit marker prior incubation with primary antibodies. Sections were incubated for 16 h at 4°C with primary antibodies; anti-CCL2 (0.4 µg/ml, Santa Cruz Biotechnology), anti-CCL7 (1 µg/ml PeproTech) and anti-PAR₁ (2 µg/ml, Santa Cruz Biotechnology). Goat and Rabbit IgG controls (Vector Laboratories) were included as a negative control. Sections were incubated for 30 min with biotin labelled anti-goat or anti-rabbit secondary antibodies (Vector Laboratories, UK), followed by 30 min incubation with ABC complex (Vector Laboratories, UK). Colour was developed with DAB chromogen (BioGenex) for 5 min. Sections were counterstained with haematoxylin, dehydrated and permanently mounted. Slides were digitally scanned using a NanoZoomer (Hamamatsu) at the equivalent of ×200 magnification.

Analysis of CCRs by flow cytometry.

Blood was isolated in heparinised tubes from naïve and LPS challenged mice. Lung was isolated and homogenised as previously described. Both tissues underwent red blood cell lysis (Roche). Leukocytes were stained with anti-Ly6G-PE monoclonal antibody (BD Biosciences, clone IA8), anti-CCR1-FITC, anti-CCR2-APC and anti-CCR3-PerCP, or anti-CXCR2-PerCP (all AbDSetotec). Neutrophils (Ly6G^{high}) were specifically gated on FSc-Ly6G^{high} and the percentage of neutrophils expressing each chemokine receptor calculated.

Isotype and fluorescence minus one controls were used to set compensations and gating strategies.

Statistical analysis.

Statistical analysis was performed using Graphpad Prism software. Comparison of more than two groups was evaluated by Two Way ANOVA. Real time PCR data was analysed by the Δ CT method. Differences in cytokine or chemokine mRNA expression, protein release or cell number between treatment groups was evaluated by One Way ANOVA with Newman-Keuls method for post hoc pair wise comparisons, by Mann-Whitney t-test or unpaired t-test with Welch's correction. A p value of less than 0.05 was considered significant.

Results

PAR₁ signalling contributes to acute lung inflammation.

In order to determine the role of PAR₁ in the early stages of acute lung inflammation, we evaluated the effect of a potent and highly selective PAR₁ antagonist (RWJ58259) following intranasal challenge with LPS (125 µg/kg). The PAR₁ antagonist was administered (5 mg/kg RWJ58259, i.p.) 30 min after LPS challenge, the dose chosen on the basis of previous reports of effective *in vivo* PAR₁ inhibition at this concentration (20, 21). As expected, LPS caused a significant increase in total cell and neutrophil recruitment into alveolar spaces after 3 h (Figure 1A and 1B), events that are indicative of the early stages of acute inflammation (24). Antagonism of PAR₁ 30 min after the onset of lung inflammation significantly decreased total cell and neutrophil numbers recruited to the airspaces (Figure 1A and 1B). Macrophage numbers in BAL fluid remained unchanged in all treatment groups, indicating that PAR₁ antagonism did not affect early macrophage recruitment (Figure 1C). The effect of PAR₁ antagonism on LPS-induced neutrophil recruitment was independently verified by flow cytometry, which demonstrated a decrease in Ly6G⁺ neutrophils recovered from BAL fluid and from whole lung homogenates (Figure 1D). Furthermore, PAR₁ antagonism resulted in decreased myeloperoxidase (MPO) levels in lung homogenates (Figure 1E). In order to examine the effect of PAR₁ antagonism on LPS-induced disruption of the alveolar-capillary barrier, serum albumin levels were measured in BAL fluid recovered from saline and LPS challenged mice. Serum albumin levels were increased in the BAL fluid of LPS challenged mice, and were significantly decreased (p=0.004) following PAR₁ antagonism (Figure 1F). These data therefore demonstrate that PAR₁ signalling influences early neutrophilic inflammation and promotes alveolar-capillary barrier disruption in a model of acute lung inflammation.

In order to assess the effect of PAR₁ antagonism on the subsequent progression of neutrophilic inflammation, mice were challenged with LPS (125 µg/kg, i.n.) followed by RWJ58259 treatment 30 min thereafter. Mice were then euthanized at 6 h and 24 h after LPS challenge and the number of BAL fluid neutrophils assessed. A single dose of PAR₁ antagonist, given 30 min after LPS challenge, reduced neutrophil accumulation at 6 h and 24 h (Figure S1). In order to determine the cellular and molecular mechanisms underlying this inflammatory process we focused on events occurring 3 h following LPS challenge.

The pro-inflammatory effects of PAR₁ signalling are mediated by the coagulation proteinase thrombin, while cytoprotective effects are mediated by activated protein C bound to its endothelial receptor EPCR (25). In order to determine the relative influence of thrombin versus APC following LPS-induced lung injury, we measured thrombin-anti-thrombin (TAT) complexes and APC in the BAL fluid and lung homogenates of control and LPS treated mice. A significant elevation of TAT was observed in the BAL fluid following LPS-challenge, but no increase in APC was observed (Figure S2). In order to rule out any effects of alternative proteinases on PAR₁ activation, the matrix metalloproteinases MMP-1 and MMP-2, and neutrophil elastase (ELA2) were measured. No differences in the expression levels of any of these proteinases were detected following LPS-challenge (Figure S2). In addition, no difference in the levels of the receptor for advanced glycation endproducts (RAGE) was detected, suggesting that epithelial cell death does not contribute to the inflammatory response during the acute phase (Figure S2).

PAR₁ signalling influences the expression of multiple inflammatory mediators.

To investigate the mechanism by which PAR₁ signalling influences acute lung inflammation, we next examined the effect of LPS challenge and subsequent PAR₁ antagonism on pro-inflammatory cytokine and neutrophil-specific chemokine levels in lung homogenates. In order to identify potential PAR₁-regulated cytokines and chemokines, we used a low density rt-PCR array to enable the profiling of 91 inflammatory mediators (Table S1). Of the 91 genes analysed, 31 genes were differentially expressed in lung tissue following challenge with LPS compared to saline treatment. The differential gene expression profile included the upregulation of several genes known to be important for the generation of inflammatory responses, such as TNF, interleukins, CXC chemokines and CC chemokines. Further analysis revealed that 13 genes exhibited decreased expression following PAR₁ antagonism (Table S1). However, PAR₁ antagonism did not attenuate the expression of the conventional pro-inflammatory cytokines TNF and IL-6 (Figure 2A and 2B), or the CXCR2 ligands CXCL1 and CXCL2 (Figure 2C and 2D), suggesting that these cytokines/chemokines are not regulated downstream of PAR₁ signalling in this model of LPS-induced lung inflammation.

Of those genes upregulated following LPS challenge, PAR₁ antagonist treatment decreased the expression of several CC and CXC chemokines, interleukins and TNF-related factors. Importantly, two closely related CC-chemokines CCL2 and CCL7 were decreased following treatment with the PAR₁ antagonist (Figure 2E and 2F). These chemokines are known to induce the egress of monocytes from the bone marrow and recruit monocytes/macrophages into inflamed tissue (14, 15). However, these chemokines are not generally considered to be major chemoattractants for neutrophils.

In order to confirm the LDA expression analysis, we measured protein levels in lung homogenates. Treatment with LPS significantly increased the expression of TNF, IL-6,

CXCL1 and CXCL2 (Figure 3A, 3B, 3C and 3D), but the expression of these proteins was not affected by PAR₁ antagonist treatment. Similarly, LPS challenge increased the expression of CCL2 and CCL7 (Figure 3E and 3F) and, as observed in the LDA rt-PCR analysis, PAR₁ antagonist treatment also decreased the expression of these chemokines at the protein level. These data provide strong support to the notion that PAR₁ plays a role in regulating CCL2 and CCL7 expression following LPS-induced lung inflammation.

CCL2 and CCL7 contribute to leukocyte accumulation following LPS challenge.

In order to examine the potential roles of CCL2 and CCL7 in LPS-induced lung inflammation, we used specific neutralizing antibodies to block these chemokines. Treatment with the CCL2 or CCL7 neutralising antibodies reduced respective chemokines to basal levels at 3 h (Figure 4A and 4B), and therefore confirmed effective target engagement. Administration of anti-CCL2 antibody significantly decreased both the total cell number and the number of neutrophils isolated from BAL fluid following challenge with LPS (Figure 4C and 4D). Neutralisation of CCL2 also decreased the number of macrophages isolated from the BAL fluid after LPS challenge (Figure 4E). Administration of anti-CCL7 antibody also significantly reduced total cell and neutrophil accumulation into airspaces following LPS challenge (Figure 4F and 4G). However, neutralisation of CCL7 did not affect the number of macrophages (Figure 4H). Taken together, these data led us to conclude that both CCL2 and CCL7 influence early neutrophil accumulation into the inflamed lung, although only CCL2 had a significant effect on the number of pulmonary macrophages.

Since LDA PCR analysis indicated that the LPS induced chemokines CXCL10 and CX3CL1 may be responsive to treatment with the PAR₁ antagonist (Table S1), *in vivo* neutralization experiments were also performed with antibodies to CXCL10 or CX3CL1. No decrease in

neutrophil accumulation was observed following neutralisation of these chemokines (Figure S3), suggesting that these chemokines are not directly involved in neutrophil migration into the LPS-inflamed lung.

CCL2, CCL7 and PAR₁ immunolocalisation in inflamed lung.

The observation that neutrophil migration downstream of PAR₁ activation was mediated by the non-classical neutrophil chemokines, CCL2 and CCL7, was unexpected. In order to determine the cellular source of these chemokines we next examined the immunolocalisation of CCL2 and CCL7 in serial lung sections from saline treated and LPS-challenged mice. Weak CCL2 staining was detected in lung sections from saline treated animals (Figure 5A). However, following LPS treatment there was increased immunolocalisation of CCL2 in bronchial epithelial cells, alveolar macrophages, and endothelial cells, and to a lesser extent alveolar epithelial cells (Figure 5B and 5C). Similarly, there was weak CCL7 staining in saline treated control lung, which was mainly restricted to the bronchial epithelium (Figure 5D), while CCL7 immunostaining of bronchial epithelial cells was markedly increased in response to LPS injury (Figure 5E and 5F). However, little immunolocalisation of CCL7 was detected in endothelial cells, alveolar epithelial cells or alveolar macrophages, suggesting that CCL2 and CCL7 are expressed within different lung microcompartments. Immunolocalisation of PAR₁ demonstrated differential expression in lung microenvironments including the bronchial epithelium and alveolar macrophages in saline treated mouse lung (Figure 5G). An increase in PAR₁ staining was detected in bronchial epithelial cells, alveolar macrophages and endothelial cells following LPS challenge (Figure 5H and 5I).

In order to gain an understanding of the relative contributions of PAR₁ and LPS signalling on the release of CCL2 and CCL7, bronchial epithelial cells (Beas2Bs) and monocytes (THP-1) were stimulated with thrombin, LPS or a combination of the two. Thrombin and LPS induced the release of CCL2 from bronchial epithelial cells, while only LPS stimulated the release of CCL2 from THP-1 cells. Neither thrombin nor LPS stimulated the release of CCL7 from either bronchial epithelial or monocytic cell lines (Figure S4). In contrast, only thrombin stimulation induced the release of IL-8 from epithelial cells, while only LPS induced the expression of IL-8 in monocytes (Figure S4). Considering thrombin and LPS were unable to stimulate CCL7 release, while CCL7 immunolocalised to the pulmonary epithelium, we next tested the effects of the classical inflammatory mediators TNF, IFN- γ or a combination of TNF and IFN- γ (cytomix) on CCL2 and CCL7 release from epithelial cells. Both TNF and IFN- γ readily induced the release of CCL2 (Figure S5). In contrast, only a combination of TNF and IFN- γ stimulation caused a substantial release of CCL7, while IFN- γ alone induced the release of a small but significant amount of CCL7 (Figure S5). In order to assess the role of IFN- γ downstream of PAR₁ *in vivo*, mice were challenged with LPS and treated with the PAR₁ antagonist RWJ58259 30 min later. However, PAR₁ antagonism had no effect on IFN- γ expression in either BAL fluid or whole lung tissues.

Neutrophils migrate into lung airspaces in response to CCL2 and CCL7.

In order to determine the whether CCL2 and CCL7 are able to directly recruit leukocytes into the lung, we next administered recombinant CCL2 or CCL7 into the lungs of naïve mice and sampled the BAL fluid after 3 h. Direct instillation of either rCCL2 or rCCL7 increased the total cell number recovered from BAL fluid compared to saline treated controls (Figure 6A). The magnitude of the response was greater for rCCL2 compared to rCCL7. Differential cell

counts revealed that administration of rCCL2 or rCCL7 resulted in the recruitment of neutrophils into lung airspaces (Figure 6B). When expressed as a percentage of total cells recovered from BAL fluid, the data revealed that rCCL7 promoted a preferential accumulation of neutrophils compared to rCCL2 (Figure 6C), although total neutrophil numbers were similar. Furthermore, rCCL2 induced the recruitment of greater numbers of monocytes/macrophages into the BAL fluid compared to rCCL7 (Figure 6D and 6E). Taken together, these data reveal that CCL2 and CCL7 attract neutrophils into the lung in the absence of any underlying inflammation, and that CCL7 preferentially promotes the recruitment of neutrophils compared to CCL2, while CCL2 recruits both high levels of both macrophages and neutrophils.

Neutrophils express CC-chemokine receptors in the inflamed lung.

In order to assess the capacity of neutrophils to respond to CC-chemokines, we next assessed the expression of the known CC-chemokine receptors CCR1, CCR2 and CCR3 by neutrophils isolated from the blood and lungs of naïve and LPS-challenged mice, and compared the expression of these receptors with the major neutrophil chemoattractant receptor CXCR2, by flow cytometry. Minimal expression of CCR1, CCR2 or CCR3 was observed on neutrophils isolated from the blood of naïve and LPS challenged mice (Figure 7A and 7B). In comparison, nearly all neutrophils isolated from the blood expressed CXCR2 (Figure 7A and 7B). A small percentage of neutrophils isolated from naïve lung expressed CCR1, CCR2 and CCR3 (Figure 7C), compared to >95% of neutrophils that expressed CXCR2 (Figure 7C). Following LPS challenge the number of neutrophils expressing CCR1 and CCR2 isolated from lung tissue increased (Figure 7D). The percentage of CCR2 expressing neutrophils, in particular, increased from ~10% in naïve lung to greater than 35%

following LPS challenge (Figure 7D). There was no change in neutrophils expressing CCR3 isolated from inflamed lung tissue compared to naïve lung (Figure 7D). Interestingly, concurrent with increased CCR1 and CCR2 expression, the percentage of CXCR2 expressing neutrophils decreased following challenge with LPS (Figure 7E). In a naïve lung >95% of neutrophils expressed CXCR2, while <60% of neutrophils expressed CXCR2 following LPS challenge, indicating that the chemokine receptor repertoire of neutrophils changes when migrating into lung tissue during an inflammatory response.

Discussion

Neutrophil accumulation at sites of inflammation is essential for the early innate immune response to infection but is also associated with sterile inflammatory events. Although an influx of neutrophils is important for the control of infection and clearance of pathogens and damaged cells, excessive neutrophilia can lead to further tissue damage and immunopathology (26). In the context of lung injury, the potentially fatal lung condition ARDS is characterised by disruption of the alveolar-capillary interface, resulting in leakage of fluid into the interstitium and alveolar compartment, and the accumulation of neutrophils within airspaces (27). Current evidence suggests that excessive neutrophil accumulation contributes to tissue damage and alveolar-capillary barrier disruption (28), and is directly associated with the severity of disease (29-31). Furthermore, alveolar-capillary barrier disruption has been directly associated with the immediate influx of neutrophils (3 h), rather than peak of influx (24 h) or secondary events of neutrophil migration (9). However, the endogenous factors and pathways that influence the rapid recruitment of neutrophils into the inflamed lung remain poorly defined. We now report that neutrophil recruitment into the lung airspaces is attenuated by antagonism of the high affinity thrombin receptor, PAR₁, in a mouse model of LPS-induced lung inflammation.

PAR₁ antagonists have been investigated extensively as potential anti-platelet agents for the treatment of thrombotic diseases. For example, RWJ-58259 significantly reduced thrombus platelet aggregation in a cynomolgus monkey model of vascular injury-induced thrombosis, by specifically targeting PAR₁ and not PAR₂₋₄ (21). The same antagonist also attenuated vascular injury in a vascular restenosis model involving balloon angioplasty in rats (20). Importantly, our *in vivo* studies used a dose of RWJ-58259 that was consistent with these previous reports. It is now recognised that the vascular barrier-modulatory effects of the

PAR₁ signalling axis are much more complex and are highly dependent on the nature and concentration of the activating proteinase. For example, at high concentrations, thrombin promotes endothelial cell contraction and vascular leak via activation of PAR₁ in association with the sphingosine-1-phosphate receptor S1P3. In contrast, both low concentrations of thrombin and activated protein C (APC) mediate barrier protective effects by signalling via PAR₁ in association with the endothelial protein C receptor (EPCR) and S1P1 (25). PAR₁ is now considered to be a receptor for danger signals, influencing the release of several pro-inflammatory mediators. Our data suggest that thrombin is the key proteinase that activates PAR₁ in this model of lung injury. Although other proteinases, such as MMP-1 and neutrophil elastase, can activate PAR₁ under certain inflammatory conditions (6, 32) these proteinases are unchanged and therefore unlikely to play a major role during the acute phase of lung inflammation in our model. Furthermore, apoptotic signals and mediators released from damaged epithelial cells are also likely to modulate the inflammatory response and contribute to the complex signalling processes that occur during lung injury (32).

Previous studies have demonstrated that PAR₁ signalling can lead to the release of certain pro-inflammatory cytokines such as TNF, IL-6 and CXCL8 (IL-8) (33-36). In the present study we now show that PAR₁ signalling influences the expression of CCL2 and CCL7, which in turn contribute to the accumulation of neutrophils into inflamed lung tissue. It is recognized that chemokines (particularly CXC chemokines) play a key role in regulating neutrophil migration into lung tissue (37, 38), and animal models of ARDS have been instrumental in revealing a central role for CXCL8 in neutrophil migration into the lung (1). There is compelling evidence that CXCL8, and the functional mouse homologues CXCL1 and CXCL2, are released by alveolar macrophages and lung epithelial cells in response to key inflammatory mediators, such as LPS, TNF and IL-1 β (39). Release of CXCL8 from

these cells establishes a chemokine gradient that not only provides neutrophils with directional movement but also delivers an activation signal that primes these cells during the process of trans-endothelial migration. Although it is clear that CXCL8 is important for the regulation of neutrophil migration (40), it is far from clear the extent to which other chemokines contribute to neutrophilic inflammation.

Previous studies have shown that neutralisation of CXCL8 in the BAL fluid of patients with mild ARDS (acute lung injury) does not completely abolish the neutrophil chemotactic activity of this fluid (10), suggesting that other chemotactic factors are present that contribute to neutrophil migration. Indeed, several other chemokines have been implicated in neutrophil migration, including CXCL10 (IP-10) (41), CXCL5 (ENA-78) (42), and CCL2 (11, 12). Taken together, these observations suggest that although classical chemoattractants such as CXCL8 (or murine CXCL1 and CXCL2) likely play key roles, neutrophils are capable of responding to a variety of chemoattractants when migrating into inflamed tissue. However, the influence that individual chemokines have on neutrophil migration is likely to be dependent on the inflammatory stimulus and the tissue in which the chemokine is acting. In the case of the lung, we would reason that tissue-specific signals within unique microenvironments may be required for effective neutrophil migration across the pulmonary capillary endothelium and alveolar epithelium.

In the present study, we now demonstrate that neutrophil migration into inflamed lung tissue following LPS challenge is mediated by CCL2 and CCL7. Indeed, we found that PAR₁ antagonism was not associated with a reduction in the expression of the classic murine neutrophil chemoattractants, CXCL1/CXCL2, following LPS-induced inflammation, but rather influenced CCL2 and CCL7 levels. The observation that PAR₁ signalling contributes to CCL2 expression in the inflamed lung is consistent with our previous findings reported in

the context of fibrotic lung injury, where we demonstrated that PAR₁ deficiency is associated with an attenuated CCL2 response in the mouse model of bleomycin-induced lung fibrosis (23, 36, 43). We now show that PAR₁ antagonism is also associated with a reduction in CCL2 and CCL7 levels, indicating that PAR₁ signalling influences the expression of two CC chemokines not commonly recognised as classical neutrophil chemoattractants. Antibody neutralization studies further revealed that CCL2 and CCL7 contribute to neutrophil accumulation in LPS-induced acute lung inflammation. It is clear from previous findings (43) that CCL2 is directly regulated by PAR₁ signalling. Immunohistochemical analysis of sections from mouse lungs challenged with LPS support this notion, as CCL2 and PAR₁ co-localised primarily to the bronchial epithelium, endothelium and alveolar macrophages. Furthermore, stimulation of bronchial epithelial cells *in vitro* with the PAR₁ activating proteinase thrombin led to increased CCL2 production. However, compared to wide-spread immunostaining observed for CCL2, CCL7 immunoreactivity was primarily restricted to the bronchial epithelium, indicating that these two chemokines are differentially expressed within specific lung microcompartments. Furthermore, in our *in vitro* studies we were unable to demonstrate a direct functional link between PAR₁ signalling and CCL7 release in either bronchial epithelial cells or monocytic cells, further supporting the notion that CCL2 and CCL7 are regulated by different signalling pathways. In contrast, a combination of TNF and IFN- γ was effective at inducing the release of CCL7, suggesting that CCL7 expression may require highly pro-inflammatory signals, the complexity of which is not easily mimicked in an *in vitro* setting. Direct instillation of rCCL2 and rCCL7 further showed that these chemokines alone can elicit neutrophil recruitment into naïve lungs. In particular, rCCL7 preferentially promoted the recruitment of neutrophils compared to CCL2, although absolute numbers recovered from BAL fluid were similar. We propose that this effect may be

explained by the greater promiscuity of CCL7, which can bind several receptors including CCR1, CCR2 and CCR3, whereas CCL2 only signals through CCR2.

CCL2 is widely regarded as a major monocyte chemoattractant, while CCL7 has previously been shown to act as a chemoattractant for several leukocyte populations including basophils, mast cells, eosinophils, DCs, T lymphocytes and monocytes/macrophages (44, 45). In particular, CCL7 has been shown to act as a monocyte chemoattractant during bone marrow egress in conjunction with CCL2, a process that is dependent on the expression of CCR2 (15). However, the function of CCL2 and CCL7 remain poorly understood during leukocyte migration into peripheral tissue and may be critically dependent on the type of inflammatory stimulus and the site of injury (28, 46, 47).

We now demonstrate that neutrophils migrating into the lung in response to LPS also upregulate CCR1 and CCR2. Conversely, CXCR2 expression was downregulated on neutrophils from inflamed lung. These studies highlight the potential of neutrophils to respond to CC-chemokines, which in turn may have important implications for the therapeutic inhibition of these receptors, and of CXCL8, in the control of neutrophilic inflammation. Studies that aim to further our understanding of neutrophil CC-chemokine receptor usage during lung inflammation are currently in progress; as it will be important to fully elucidate the dynamics of neutrophil recruitment with respect to the acquisition of novel chemokine receptors within different tissue microenvironments.

In conclusion, we provide strong support that PAR₁ signalling contributes to alveolar-capillary barrier disruption and neutrophil accumulation following LPS-induced lung inflammation by influencing the levels of the CC-chemokines CCL2 and CCL7. Our findings further suggest that CCL2 and CCL7 are not only differentially regulated by disparate signalling pathways within specific lung microenvironments, but that they also differentially

influence the recruitment of inflammatory leukocytes, albeit with overlapping functional modalities. Achieving the appropriate balance of reducing excessive neutrophil accumulation without impacting host innate immune function represents a major challenge for the treatment of acute and chronic inflammatory conditions. Modulating this CC-chemokine response via antagonism of PAR₁ signalling, or by blocking these chemokines directly, may represent novel opportunities for interfering with excessive neutrophilia and tissue damage in diseases such as ARDS and potentially other conditions associated with acute neutrophilic inflammation. In terms of strategies aimed at inhibiting PAR₁ signalling, PAR₁ antagonists are currently being evaluated as novel anti-thrombotic agents in several large multi-centre trials (48, 49). Our findings provide support for extending the evaluation of these agents in the context of ARDS and potentially other acute neutrophilic inflammatory conditions.

Reference List

1. Grommes J, Soehnlein O. Contribution of Neutrophils to Acute Lung Injury. *Mol Med* 2011;17:293-307.
2. Chambers RC. Procoagulant Signalling Mechanisms in Lung Inflammation and Fibrosis: Novel Opportunities for Pharmacological Intervention? *Br J Pharmacol* 2008;153 Suppl 1:S367-S378.
3. Howell DC, Laurent GJ, Chambers RC. Role of Thrombin and Its Major Cellular Receptor, Protease-Activated Receptor-1, in Pulmonary Fibrosis. *Biochem Soc Trans* 2002;30:211-216.
4. Jenkins RG, Su X, Su G, Scotton CJ, Camerer E, Laurent GJ, Davis GE, Chambers RC, Matthay MA, Sheppard D. Ligation of Protease-Activated Receptor 1 Enhances Alpha(v)Beta6 Integrin-Dependent TGF-Beta Activation and Promotes Acute Lung Injury. *J Clin Invest* 2006;116:1606-1614.
5. Scotton CJ, Krupiczko MA, Konigshoff M, Mercer PF, Lee YC, Kaminski N, Morser J, Post JM, Maher TM, Nicholson AG, et al. Increased Local Expression of Coagulation Factor X Contributes to the Fibrotic Response in Human and Murine Lung Injury. *J Clin Invest* 2009;119:2550-2563.
6. Tressel SL, Kaneider NC, Kasuda S, Foley C, Koukos G, Austin K, Agarwal A, Covic L, Opal SM, Kuliopulos A. A Matrix Metalloprotease-PAR1 System Regulates Vascular Integrity, Systemic Inflammation and Death in Sepsis. *EMBO Mol Med* 2011;3:370-384.

7. Levitt JE, Gould MK, Ware LB, Matthay MA. The Pathogenetic and Prognostic Value of Biologic Markers in Acute Lung Injury. *J Intensive Care Med* 2009;24:151-167.
8. Chambers RC. Role of Coagulation Cascade Proteases in Lung Repair and Fibrosis. *Eur Respir J Suppl* 2003;44:33s-35s.
9. Chignard M, Balloy V. Neutrophil Recruitment and Increased Permeability During Acute Lung Injury Induced by Lipopolysaccharide. *Am J Physiol Lung Cell Mol Physiol* 2000;279:L1083-L1090.
10. Miller EJ, Cohen AB, Nagao S, Griffith D, Maunder RJ, Martin TR, Weiner-Kronish JP, Sticherling M, Christophers E, Matthay MA. Elevated Levels of NAP-1/Interleukin-8 Are Present in the Airspaces of Patients With the Adult Respiratory Distress Syndrome and Are Associated With Increased Mortality. *Am Rev Respir Dis* 1992;146:427-432.
11. Balamayooran G, Batra S, Balamayooran T, Cai S, Jeyaseelan S. Monocyte Chemoattractant Protein 1 Regulates Pulmonary Host Defense Via Neutrophil Recruitment During Escherichia Coli Infection. *Infect Immun* 2011;79:2567-2577.
12. Balamayooran G, Batra S, Theivanthiran B, Cai S, Pacher P, Jeyaseelan S. Intrapulmonary G-CSF Rescues Neutrophil Recruitment to the Lung and Neutrophil Release to Blood in Gram-Negative Bacterial Infection in MCP-1^{-/-} Mice. *J Immunol* 2012;189:5849-5859.
13. Crane MJ, Hokeness-Antonelli KL, Salazar-Mather TP. Regulation of Inflammatory Monocyte/Macrophage Recruitment From the Bone Marrow During Murine

Cytomegalovirus Infection: Role for Type I Interferons in Localized Induction of CCR2 Ligands. *J Immunol* 2009;183:2810-2817.

14. Tsou CL, Peters W, Si Y, Slaymaker S, Aslanian AM, Weisberg SP, Mack M, Charo IF. Critical Roles for CCR2 and MCP-3 in Monocyte Mobilization From Bone Marrow and Recruitment to Inflammatory Sites. *J Clin Invest* 2007;117:902-909.
15. Jia T, Serbina NV, Brandl K, Zhong MX, Leiner IM, Charo IF, Pamer EG. Additive Roles for MCP-1 and MCP-3 in CCR2-Mediated Recruitment of Inflammatory Monocytes During *Listeria Monocytogenes* Infection. *J Immunol* 2008;180:6846-6853.
16. Winter C, Herbold W, Maus R, Langer F, Briles DE, Paton JC, Welte T, Maus UA. Important Role for CC Chemokine Ligand 2-Dependent Lung Mononuclear Phagocyte Recruitment to Inhibit Sepsis in Mice Infected With *Streptococcus Pneumoniae*. *J Immunol* 2009;182:4931-4937.
17. Kurihara T, Warr G, Loy J, Bravo R. Defects in Macrophage Recruitment and Host Defense in Mice Lacking the CCR2 Chemokine Receptor. *J Exp Med* 1997;186:1757-1762.
18. Zhang HC, Derian CK, Andrade-Gordon P, Hoekstra WJ, McComsey DF, White KB, Poulter BL, Addo MF, Cheung WM, Damiano BP, et al. Discovery and Optimization of a Novel Series of Thrombin Receptor (Par-1) Antagonists: Potent, Selective Peptide Mimetics Based on Indole and Indazole Templates. *J Med Chem* 2001;44:1021-1024.

19. Damiano BP, Derian CK, Maryanoff BE, Zhang HC, Gordon PA. RWJ-58259: a Selective Antagonist of Protease Activated Receptor-1. *Cardiovasc Drug Rev* 2003;21:313-326.
20. Andrade-Gordon P, Derian CK, Maryanoff BE, Zhang HC, Addo MF, Cheung W, Damiano BP, D'Andrea MR, Darrow AL, de GL, et al. Administration of a Potent Antagonist of Protease-Activated Receptor-1 (PAR-1) Attenuates Vascular Restenosis Following Balloon Angioplasty in Rats. *J Pharmacol Exp Ther* 2001;298:34-42.
21. Derian CK, Damiano BP, Addo MF, Darrow AL, D'Andrea MR, Nedelman M, Zhang HC, Maryanoff BE, Andrade-Gordon P. Blockade of the Thrombin Receptor Protease-Activated Receptor-1 With a Small-Molecule Antagonist Prevents Thrombus Formation and Vascular Occlusion in Nonhuman Primates. *J Pharmacol Exp Ther* 2003;304:855-861.
22. Ramachandran R, Noorbakhsh F, Defea K, Hollenberg MD. Targeting Proteinase-Activated Receptors: Therapeutic Potential and Challenges. *Nat Rev Drug Discov* 2011;11:69-86.
23. Howell DC, Johns RH, Lasky JA, Shan B, Scotton CJ, Laurent GJ, Chambers RC. Absence of Proteinase-Activated Receptor-1 Signaling Affords Protection From Bleomycin-Induced Lung Inflammation and Fibrosis. *Am J Pathol* 2005;166:1353-1365.
24. Summers C, Rankin SM, Condliffe AM, Singh N, Peters AM, Chilvers ER. Neutrophil Kinetics in Health and Disease. *Trends Immunol* 2010;31:318-324.

25. Ma L, Dorling A. The Roles of Thrombin and Protease-Activated Receptors in Inflammation. *Semin Immunopathol* 2012;34:63-72.
26. Sadik CD, Kim ND, Luster AD. Neutrophils Cascading Their Way to Inflammation. *Trends Immunol* 2011;32:452-460.
27. Matute-Bello G, Downey G, Moore BB, Groshong SD, Matthay MA, Slutsky AS, Kuebler WM. An Official American Thoracic Society Workshop Report: Features and Measurements of Experimental Acute Lung Injury in Animals. *Am J Respir Cell Mol Biol* 2011;44:725-738.
28. Maus U, von GK, Kuziel WA, Mack M, Miller EJ, Cihak J, Stangassinger M, Maus R, Schlondorff D, Seeger W, et al. The Role of CC Chemokine Receptor 2 in Alveolar Monocyte and Neutrophil Immigration in Intact Mice. *Am J Respir Crit Care Med* 2002;166:268-273.
29. Wiedermann FJ, Mayr AJ, Kaneider NC, Fuchs D, Mutz NJ, Schobersberger W. Alveolar Granulocyte Colony-Stimulating Factor and Alpha-Chemokines in Relation to Serum Levels, Pulmonary Neutrophilia, and Severity of Lung Injury in ARDS. *Chest* 2004;125:212-219.
30. Aggarwal A, Baker CS, Evans TW, Haslam PL. G-CSF and IL-8 but Not GM-CSF Correlate With Severity of Pulmonary Neutrophilia in Acute Respiratory Distress Syndrome. *Eur Respir J* 2000;15:895-901.
31. Matthay MA. Cellular Basis for Injury and Repair in the Adult Respiratory Distress Syndrome. *West J Med* 1985;143:665-667.

32. Suzuki T, Yamashita C, Zemans RL, Briones N, Van LA, Downey GP. Leukocyte Elastase Induces Lung Epithelial Apoptosis Via a PAR-1-, NF-KappaB-, and P53-Dependent Pathway. *Am J Respir Cell Mol Biol* 2009;41:742-755.
33. Wang L, Luo J, Fu Y, He S. Induction of Interleukin-8 Secretion and Activation of ERK1/2, P38 MAPK Signaling Pathways by Thrombin in Dermal Fibroblasts. *Int J Biochem Cell Biol* 2006;38:1571-1583.
34. Scholz M, Vogel JU, Hover G, Kotchetkov R, Cinatl J, Doerr HW, Cinatl J. Thrombin Stimulates IL-6 and IL-8 Expression in Cytomegalovirus-Infected Human Retinal Pigment Epithelial Cells. *Int J Mol Med* 2004;13:327-331.
35. Asokanathan N, Graham PT, Fink J, Knight DA, Bakker AJ, McWilliam AS, Thompson PJ, Stewart GA. Activation of Protease-Activated Receptor (PAR)-1, PAR-2, and PAR-4 Stimulates IL-6, IL-8, and Prostaglandin E2 Release From Human Respiratory Epithelial Cells. *J Immunol* 2002;168:3577-3585.
36. Deng X, Mercer PF, Scotton CJ, Gilchrist A, Chambers RC. Thrombin Induces Fibroblast CCL2/JE Production and Release Via Coupling of PAR1 to Galphaq and Cooperation Between ERK1/2 and Rho Kinase Signaling Pathways. *Mol Biol Cell* 2008;19:2520-2533.
37. Goodman RB, Pugin J, Lee JS, Matthay MA. Cytokine-Mediated Inflammation in Acute Lung Injury. *Cytokine Growth Factor Rev* 2003;14:523-535.
38. Pease JE, Sabroe I. The Role of Interleukin-8 and Its Receptors in Inflammatory Lung Disease: Implications for Therapy. *Am J Respir Med* 2002;1:19-25.

39. Mukaida N. Pathophysiological Roles of Interleukin-8/CXCL8 in Pulmonary Diseases. *Am J Physiol Lung Cell Mol Physiol* 2003;284:L566-L577.
40. Harada A, Sekido N, Akahoshi T, Wada T, Mukaida N, Matsushima K. Essential Involvement of Interleukin-8 (IL-8) in Acute Inflammation. *J Leukoc Biol* 1994;56:559-564.
41. Ichikawa A, Kuba K, Morita M, Chida S, Tezuka H, Hara H, Sasaki T, Ohteki T, Ranieri VM, Dos Santos CC, et al. CXCL10-CXCR3 Enhances the Development of Neutrophil-Mediated Fulminant Lung Injury of Viral and Nonviral Origin. *Am J Respir Crit Care Med* 2013;187:65-77.
42. Bozic CR, Gerard NP, Gerard C. Receptor Binding Specificity and Pulmonary Gene Expression of the Neutrophil-Activating Peptide ENA-78. *Am J Respir Cell Mol Biol* 1996;14:302-308.
43. Mercer PF, Johns RH, Scotton CJ, Krupiczkoj MA, Konigshoff M, Howell DC, McAnulty RJ, Das A, Thorley AJ, Tetley TD, et al. Pulmonary Epithelium Is a Prominent Source of Proteinase-Activated Receptor-1-Inducible CCL2 in Pulmonary Fibrosis. *Am J Respir Crit Care Med* 2009;179:414-425.
44. Menten P, Wuyts A, Van DJ. Monocyte Chemotactic Protein-3. *Eur Cytokine Netw* 2001;12:554-560.
45. Van DJ, Proost P, Lenaerts JP, Opdenakker G. Structural and Functional Identification of Two Human, Tumor-Derived Monocyte Chemotactic Proteins (MCP-2 and MCP-3) Belonging to the Chemokine Family. *J Exp Med* 1992;176:59-65.

46. Saban R, D'Andrea MR, Andrade-Gordon P, Derian CK, Dozmorov I, Ihnat MA, Hurst RE, Simpson C, Saban MR. Regulatory Network of Inflammation Downstream of Proteinase-Activated Receptors. *BMC Physiol* 2007;7:3.
47. Maus UA, Waelsch K, Kuziel WA, Delbeck T, Mack M, Blackwell TS, Christman JW, Schlondorff D, Seeger W, Lohmeyer J. Monocytes Are Potent Facilitators of Alveolar Neutrophil Emigration During Lung Inflammation: Role of the CCL2-CCR2 Axis. *J Immunol* 2003;170:3273-3278.
48. The Thrombin Receptor Antagonist for Clinical Event Reduction in Acute Coronary Syndrome (TRA*CER) Trial: Study Design and Rationale. *Am Heart J* 2009;158:327-334.
49. Morrow DA, Scirica BM, Fox KA, Berman G, Strony J, Veltri E, Bonaca MP, Fish P, McCabe CH, Braunwald E. Evaluation of a Novel Antiplatelet Agent for Secondary Prevention in Patients With a History of Atherosclerotic Disease: Design and Rationale for the Thrombin-Receptor Antagonist in Secondary Prevention of Atherothrombotic Ischemic Events (TRA 2 Degrees P)-TIMI 50 Trial. *Am Heart J* 2009;158:335-341.

Footnotes.

Funding: This work was supported by funding from the Medical Research Council UK (Grant numbers G0800265 and G0800340), Wellcome Trust, as well as the Rosetrees Trust. LDA analysis was supported by funding from Centocor Inc. This work was supported by funding from the Medical Research Council (UK) Grant numbers G0800265 and G0800340. Support was also received from Centocor Inc, and the Rosetrees Trust.

Competing interests: RCC, PFM and AEW have filed a patent on PAR-1 and CCL7 as novel drug targets in acute lung injury.

Figure Legends.

Figure 1. PAR₁ antagonist treatment significantly attenuates LPS induced lung injury.

Mice were euthanized 3 hours after LPS (125 µg/kg i.n.) or saline challenge with or without the highly selective PAR₁ antagonist RWJ-58259 (5 mg/kg) dosed therapeutically (i.p.) after 30 min. Lungs were lavaged (1.5 ml PBS total) or removed and homogenised for FACS analysis. Total (A) and differential BAL fluid neutrophils (B) were quantified by haemocytometer and cyospin counts. BAL fluid macrophages were also differentially counted from cyospin preparations (E). Ly6G⁺ neutrophils (Ly6G^{high} F4/80^{low/neg}) isolated from BAL fluid or lung homogenates were further assessed by flow cytometry (D). Neutrophil myeloperoxidase (MPO) activity in lung homogenates was assessed by ELISA (E). Alveolar-capillary barrier permeability was measured as serum albumin in BAL fluid by ELISA (F). Panel shows mean values for at least n=5/group from three separate experiments. Data were analysed by one way ANOVA with Newman-Keuls Post Hoc test: ***p<0.0001, **p<0.01, *p<0.05.

Figure 2. Low density array analysis of inflammatory markers following PAR₁ antagonism.

Mice were euthanized 3 hours after LPS (125 µg/kg i.n.) or saline challenge with or without the the highly selective PAR₁ antagonist RWJ-58259 (5 mg/kg) dosed therapeutically (i.p.) after 30 min. Lungs were removed, snap frozen and homogenised under liquid nitrogen before RNA was isolated and run on a low density gene array consisting of 151 inflammatory markers (Supplementary table 1). Gene expression following LPS treatment revealed 25 markers that exhibited reduced expression following PAR₁ antagonism. Of these genes the pro-inflammatory cytokines TNF (A) and IL-6 (B), and the neutrophil

chemoattractants CXCL1 (C) and CXCL2 (D) are depicted. In addition, the chemokines CCL2 (E) and CCL7 (F) were measured. Panel shows mean values for at least n=5/group from three separate experiments. Data were analysed by one way ANOVA with Newman-Keuls Post Hoc test: **p<0.01, *p<0.05.

Figure 3. PAR₁ antagonist treatment decreases CCL2 and CCL7 expression. Mice were euthanized three hours after LPS (125 µg/kg i.n.) or saline challenge with or without the PAR₁ antagonist RWJ-58259 (5 mg/kg) dosed i.p. after 30 min. Lungs were removed and homogenized. Levels of TNF (A), IL-6 (B) CXCL1 (C), and CXCL2 (D) protein were measured in lung homogenates using a Luminex bead array. Protein levels of CCL2 (H) and CCL7 (I) were measured from lung homogenates by ELISA. Panel shows mean values for at least n=5/group from three separate experiments. Data were analysed by one way ANOVA with Newman-Keuls post hoc test: ***p<0.001, **p<0.01, *p<0.05.

Figure 4. CC-chemokines influence early leukocyte accumulation in response to LPS challenge. Mice were euthanized three hours after LPS (125 µg/kg i.n.) or saline challenge. Mice were administered with anti-CCL2 or anti-CCL7 neutralising antibody (10 µg/mouse), or control IgG, within the nasal challenge volume. Lungs were removed, homogenised and CCL2 (A) and CCL7 (B) levels measured by ELISA following anti-CCL2 or anti-CCL7 antibody treatment. Lungs were lavaged and BAL fluid total cells (C), neutrophils (D) and macrophages (E) quantified following administration of anti-CCL2. Following anti-CCL7 treatment lungs were lavaged and BAL fluid total cells (F), neutrophils (G) and macrophages (H) quantified. Mean and sem values of at least n=5 per group for 2 separate experiments are

shown for each treatment. Data were analysed by one way ANOVA with Newman-Keuls post hoc test: $**p<0.01$, $*p<0.05$; n.s. not significant.

Figure 5. Immunohistochemical analysis of CCL2, CCL7 and PAR₁ expression in the lungs of LPS-treated mice. Mice were euthanized three hours after LPS (125 µg/kg i.n.) or saline challenge. Lungs were inflated with 4% formaldehyde and serial paraffin embedded sections (4 µm) cut. Immunohistochemistry was performed on each section to detect CCL2 (A, B and C), CCL7 (D, E and F) or PAR₁ (G, H and I). Images were digitally captured using a NanoZoomer (Hamamatsu) at the equivalent of ×200 magnification. High magnification images were taken of LPS-treated lungs equivalent to ×400 magnification (C, F and I). Images are representative of 5 mice per treatment group.

Figure 6. CCL2 and CCL7 induce an influx of leukocytes into the BAL fluid. Naïve mice were administered with either rCCL2 or rCCL7 (500 ng/mouse, i.n.) and 3 h later BAL fluid was recovered. BAL fluid total cell counts (A) were measured following rCCL2 and rCCL7 treatment. Differential cell counts were performed on isolated BALF by cytopsin. The total number of neutrophils (B) and the percentage of neutrophils (C) in BAL fluid were calculated. In addition, the total number of macrophages (D) and the percentage of macrophages (E) in BAL fluid were calculated. Data were analysed by one way ANOVA with Newman-Keuls post hoc test: $*p<0.05$, $**p<0.01$, $***p<0.001$.

Figure 7. CC-chemokine receptor expression of neutrophils isolated from the blood and lung. Mice were administered with LPS (125 µg/kg i.n.) or without (naïve) and blood and lungs isolated and single cell suspensions prepared. Cells were stained for Ly6G and the

neutrophil population specifically gated (Ly6G^{high} against FSc). The expression of CCR1, CCR2, CCR3 and CXCR2 on neutrophils was calculated and represented as dot plots. Neutrophils isolated from naïve blood (A), LPS treated blood (B), naïve lungs (C) and LPS-treated lungs (D) were analysed and the percentage of chemokine receptor positive cells calculated (E). Data are representative of 5 mice per group. Data were analysed by one way ANOVA with Newman-Keuls post hoc test: $*p < 0.05$ compared to naïve blood.

Figure 1

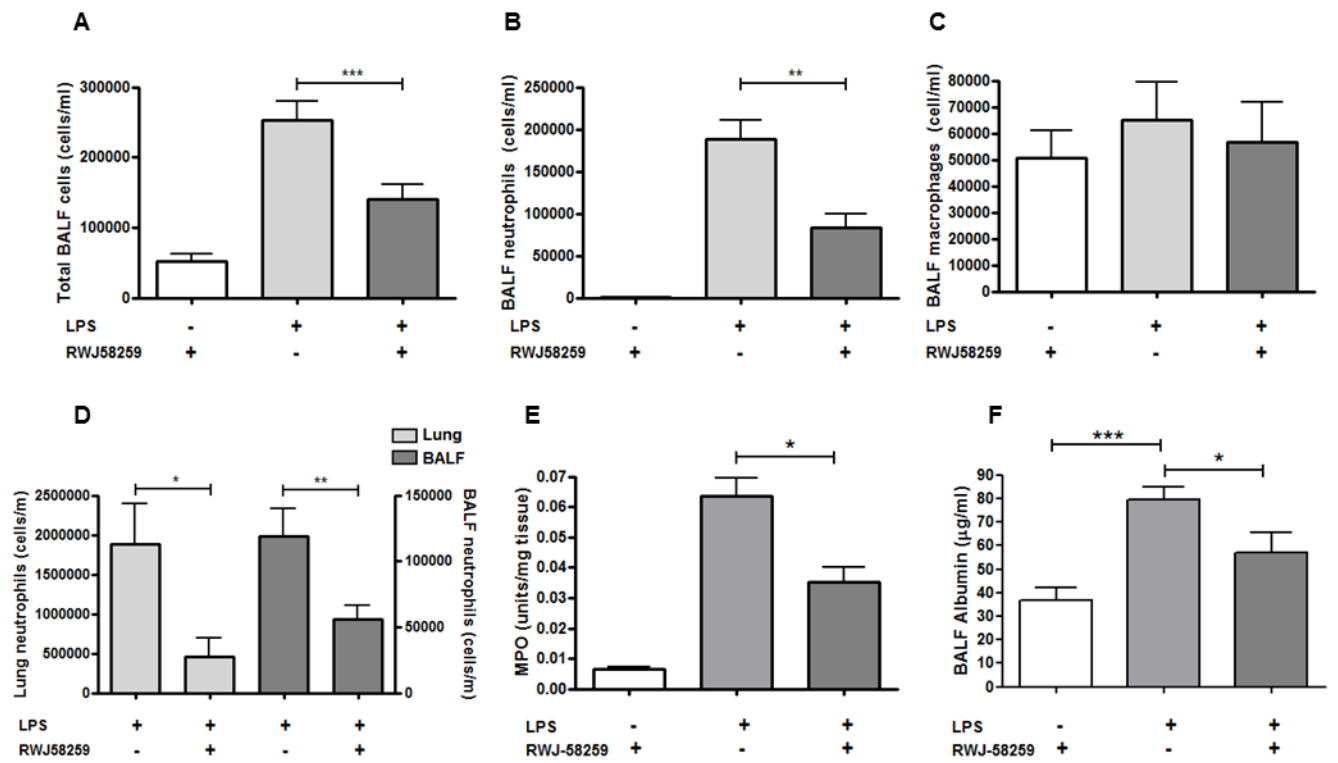


Figure 2.

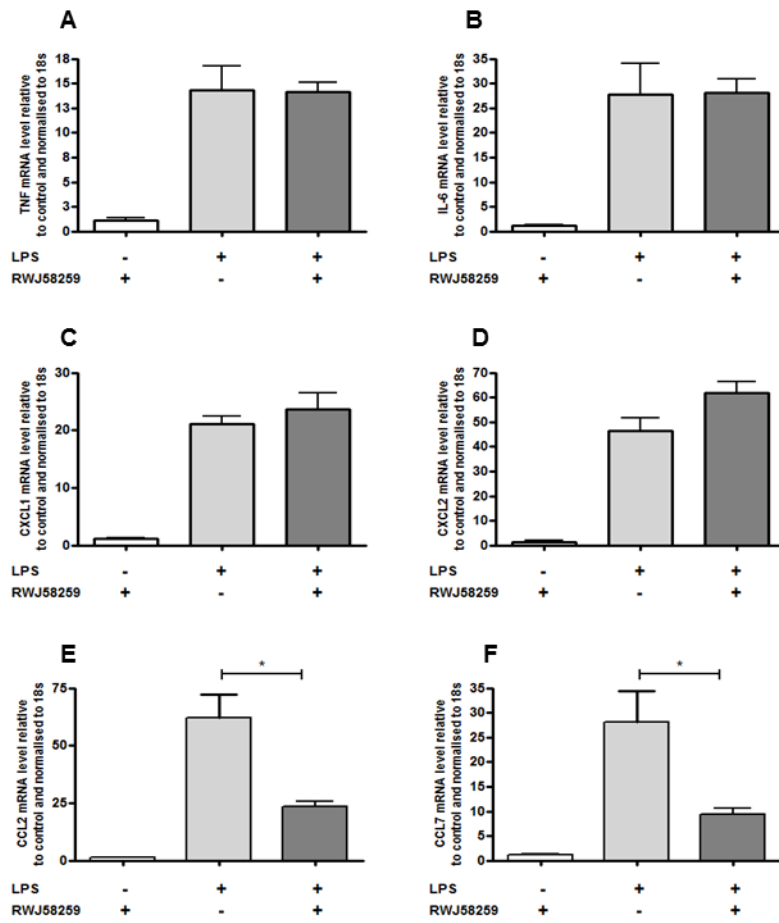


Figure 3.

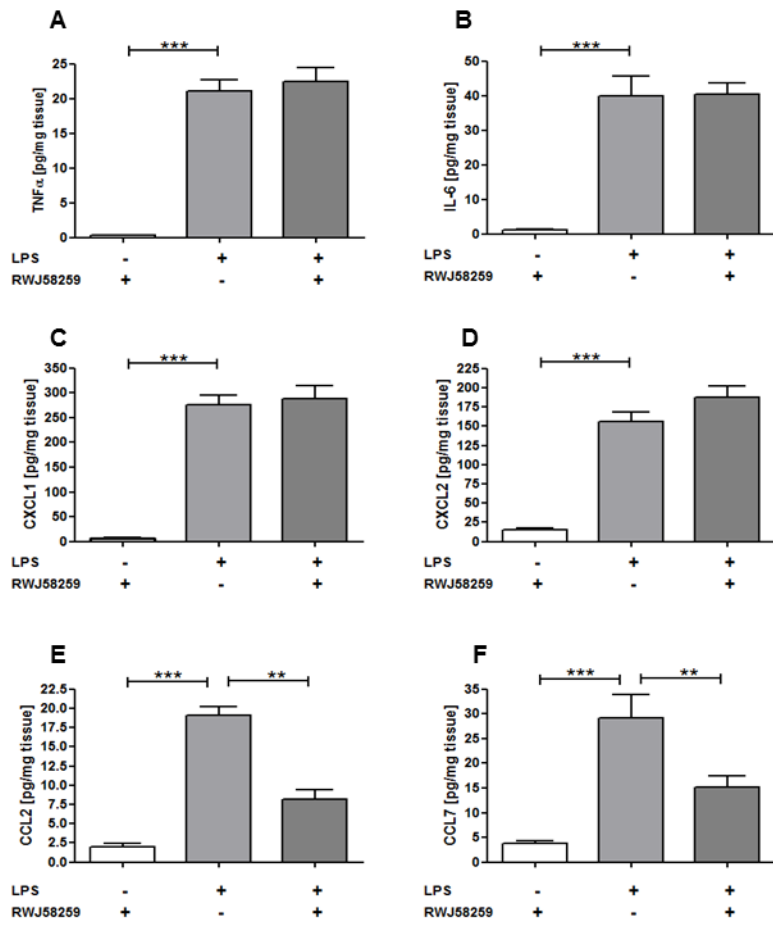


Figure 4.

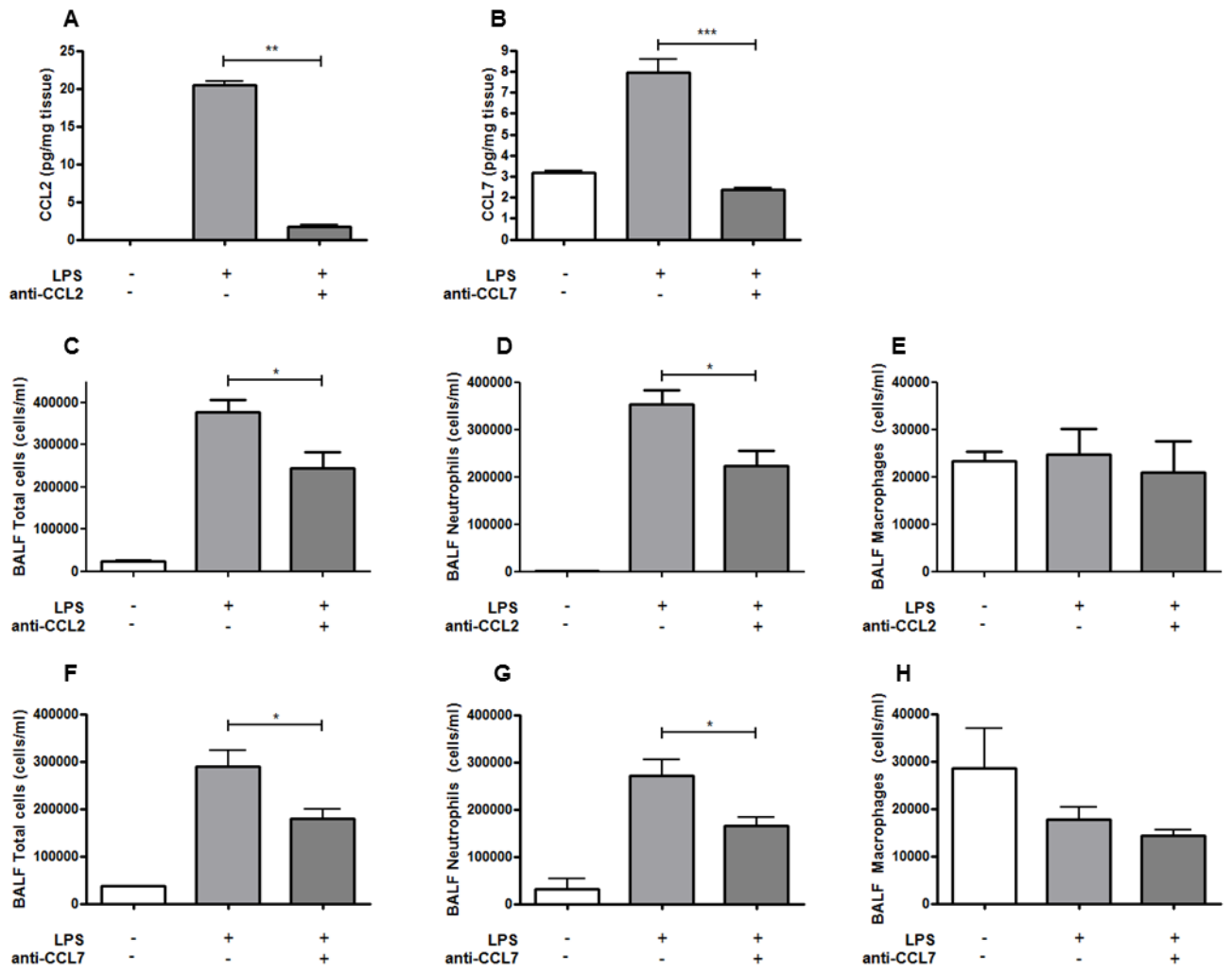


Figure 5.

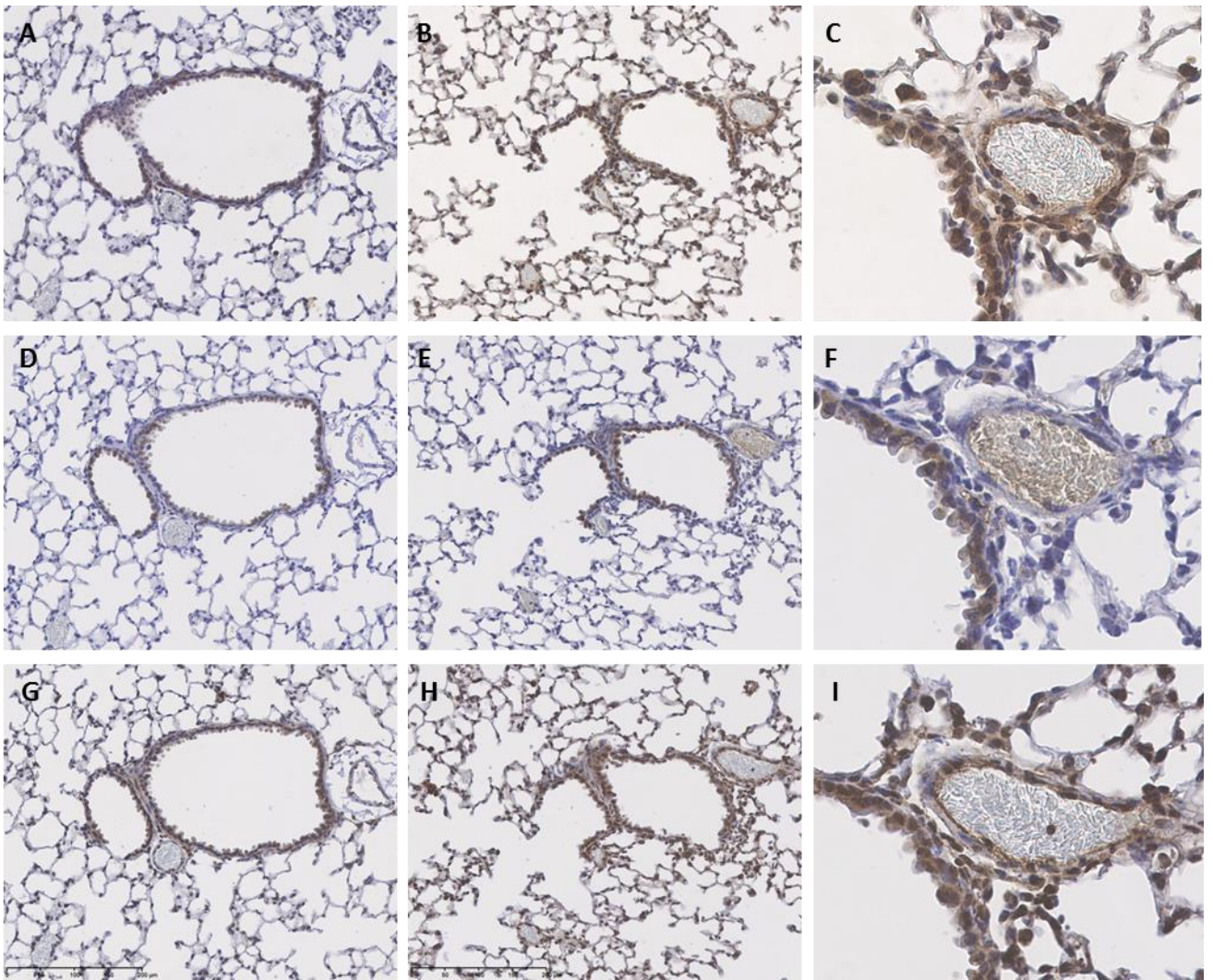


Figure 6.

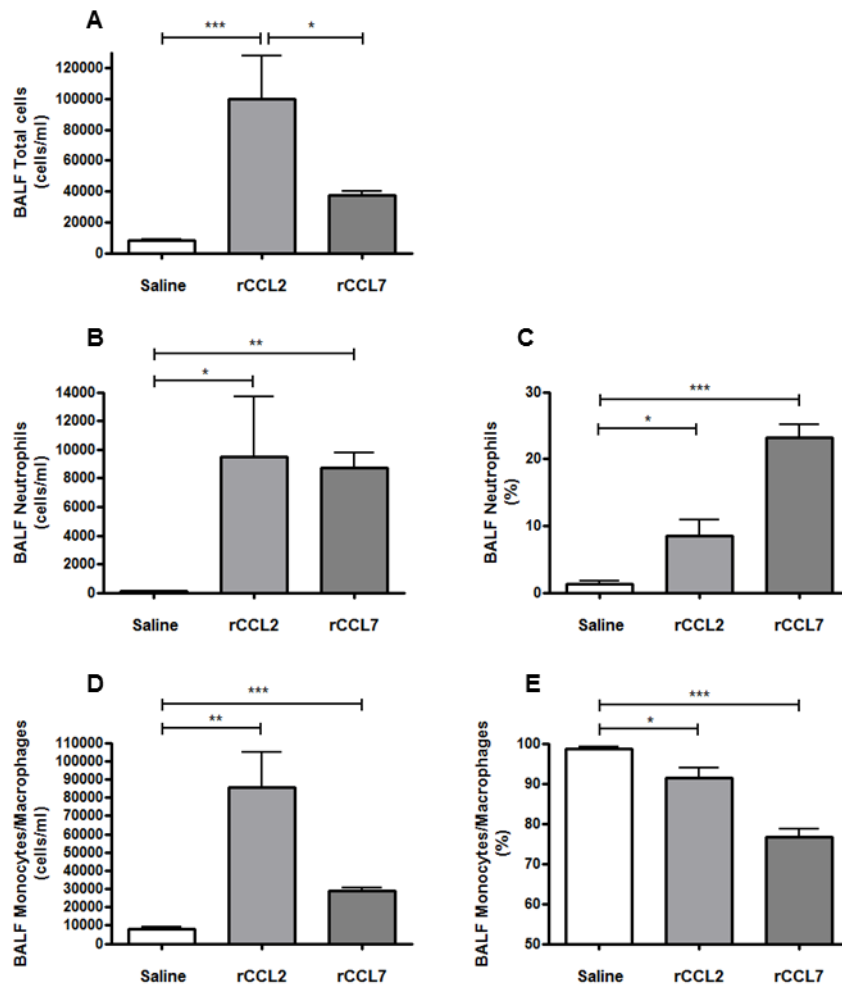


Figure 7.

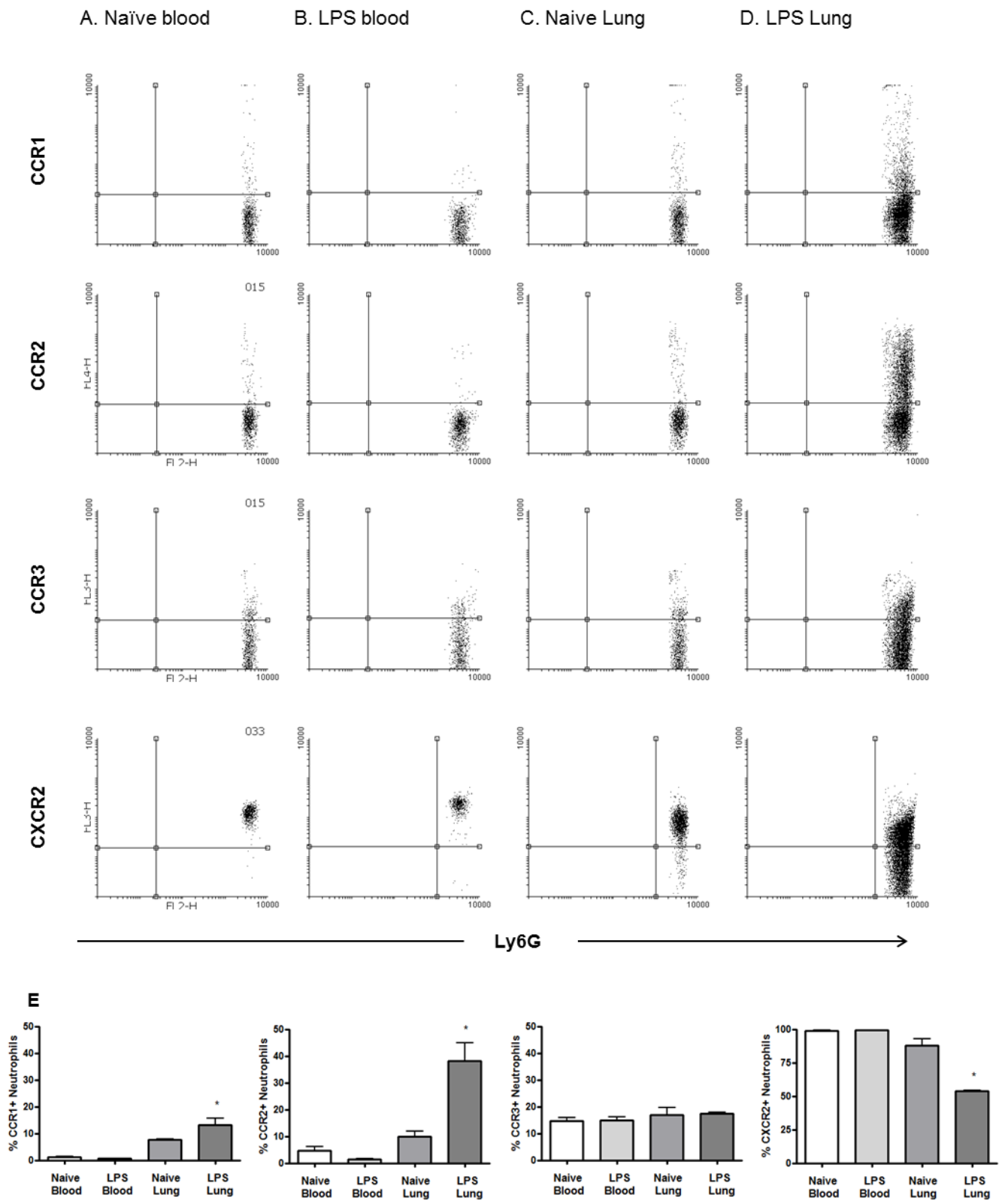


Fig. S1. PAR₁ antagonism moderates airspace neutrophilia after 6 and 24 h. Mice were euthanized 6 h or 24 h after LPS (125 μ g/kg i.n.) or saline challenge with and without the

PAR₁ antagonist RWJ-58259 (5 mg/kg) dosed therapeutically (i.p) after 30 min. Lungs were lavaged (1.5 ml PBS total) and the neutrophils counts after 6 h (A) and 24 h (B). Data were analysed by one way ANOVA with Neuman-Keuls Post Hoc test: * $p < 0.05$.

Fig. S2. Elevated levels of thrombin-anti-thrombin (TAT) complex in inflamed airspaces. Mice were euthanized 3 h after LPS (125 µg/kg i.n.) or saline challenge. BAL fluid was isolated and the levels of TAT (A) and APC (B) measured. Whole lung tissue was homogenised and the levels of TAT (C), APC (D), MMP1 (E), MMP2 (F), neutrophil elastase (ELA2) (G) and receptor for advanced glycation end products (RAGE) (H) measured by ELISA.

Fig. S3. Neutralisation of CXCL10 and CX3CR1 did not result in a decrease in airspace neutrophilia. Mice were euthanized three hours after LPS (125 µg/kg i.n.) challenge with or without PAR₁ antagonist. LDA analysis of CXCL10 (A) and CX3CL1 (B) mRNA levels (normalised to 18s housekeeping gene). Mice were administered CXCL10 or CX3CL1 neutralising antibody (10 µg/mouse) within the LPS nasal challenge volume. Lungs were lavaged (1.5 ml PBS total) and differential BAL fluid neutrophils quantified following administration of anti-CXCL10 (C) or anti-CX3CL1 (D) neutralising antibodies. Data were analysed by one way ANOVA with Neuman Keuls post hoc test. ** $p < 0.01$.

Fig. S4. The expression of CCL2, CCL7 and IL-8 is differentially induced by thrombin and LPS. The bronchial epithelial cell line Beas2B and the macrophage cell line THP-1 were stimulated with thrombin (10 nM), LPS (100 ng/ml) or a combination of the two. The levels of CCL2 expressed by epithelial cells (A) or macrophages (B) were measured by ELISA. Similarly, the levels of CCL7 expressed by epithelial cells (C) or macrophages (D) were

measured by ELISA. IL-8 levels were also measured following stimulation of epithelial cells (E) and macrophages (F). Data were analysed by unpaired t-test with Welch's correction (*p<0.05 compared to media control).

Fig. S5. CCL7 is expressed in response to TNF and IFN- γ . The bronchial epithelial cell line Beas2B was stimulated with TNF (20 ng/ml), IFN- γ (20 ng/ml) or a combination of both. CCL2 (A) and CCL7 (B) levels were measured by ELISA. Data were analysed by unpaired t-test with Welch's correction (*p<0.05 compared to media control). In separate experiments mice were euthanized 3 h after LPS (125 μ g/kg i.n.) or saline challenge. The expression of IFN- γ in isolated BAL fluid (C) and whole lung homogenates (D) was measured by ELISA. Data were analysed by unpaired t-test with Welch's correction (*p=0.03)

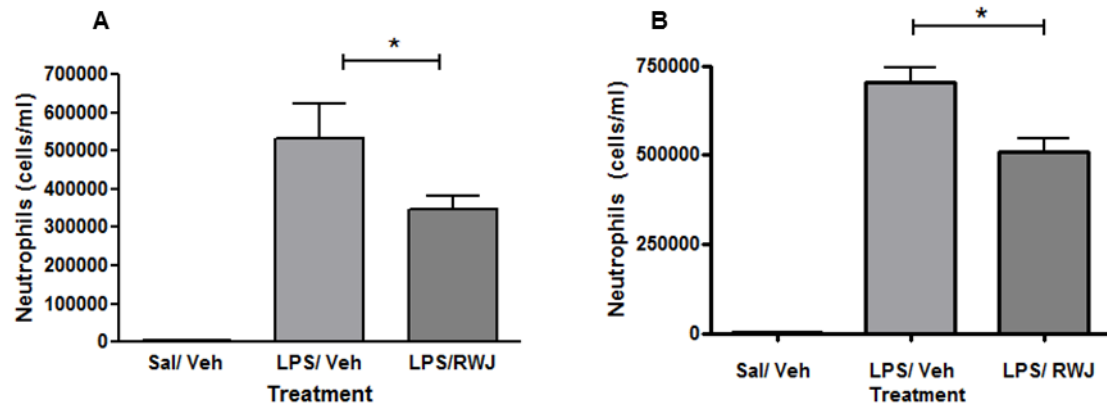
Supplementary Table S1. Low density PCR array raw data.

Gene	Challenge/ Treatment								
	Saline/ Vehicle		LPS/ Vehicle		LPS/ Veh vs Sal/ Veh (p-value)	LPS/ RWJ58259		LPS/ RWJ vs Sal/ Veh (p value)	LPS/ Veh vs LPS/ RWJ (p value)
	Mean	sem	Mean	sem		Mean	sem		
Ccl 2	1.49	0.52	62.51	10.63	<0.0001	26.70	2.52	<0.0001	<0.05
Ccl 3	1.12	0.29	41.03	9.13	<0.0001	31.86	1.98	<0.0001	ns
Ccl 4	1.04	0.15	55.02	7.37	<0.0001	50.40	2.71	<0.0001	ns
Ccl 7	1.11	0.20	28.19	6.14	<0.0001	9.33	1.34	<0.0001	<0.01
Ccl 11	1.02	0.11	5.65	0.92	<0.0001	4.53	0.31	<0.0001	ns
Ccl 17	1.11	0.25	16.18	2.64	<0.0001	18.59	1.86	<0.0001	ns
Ccl 22	1.04	0.14	28.90	6.85	<0.0001	18.39	1.63	<0.0001	ns
Cxcl 1	1.10	0.27	21.09	1.36	<0.0001	23.68	2.84	<0.0001	ns
Cxcl 2	1.44	0.62	46.46	5.18	<0.0001	61.90	4.45	<0.0001	ns
Cxcl 10	1.07	0.18	279.23	62.16	<0.0001	149.68	14.79	<0.0001	<0.05
Cxcl 13	1.05	0.16	5.49	0.89	<0.0001	5.00	0.82	<0.0001	ns
Cx3cl 1	1.01	0.07	3.15	0.62	<0.0001	1.42	0.07	<0.05	<0.0001
Ccr 1	1.04	0.15	6.62	1.10	<0.0001	5.54	0.75	<0.0001	ns
Ccr 3	1.06	0.19	0.83	0.20		0.28	0.04		
Ccr 4	1.20	0.34	2.92	0.75	<0.05	1.21	0.12	ns	<0.05
Ccr 7	1.03	0.14	1.29	0.22		0.93	0.11		
Ccr 8	1.21	0.42	1.82	0.48		2.16	0.48		
CXCR 2	1.08	0.21	13.42	2.52	<0.0001	12.53	1.49	<0.0001	ns
Cxcr 3	1.07	0.21	0.60	0.05		0.58	0.08		
CXCR 5	1.04	0.15	0.92	0.18	ns	0.48	0.04	<0.05	<0.05
Cxcr 6	1.38	0.38	2.00	0.51		1.17	0.21		
Bmp7	1.02	0.10	0.64	0.06	<0.01	0.51	0.07	<0.01	ns
Col1a1	1.04	0.13	0.72	0.11	ns	0.47	0.03	<0.01	<0.05
Csf2	1.11	0.28	18.25	1.87	<0.0001	14.00	2.63	<0.0001	ns
Csf3	2.55	1.12	81.97	17.57	<0.0001	133.70	9.08	<0.0001	ns
Ctgf	1.04	0.16	0.61	0.10	<0.05	0.54	0.07	<0.05	ns
Ddr1	2.02	0.92	4.37	1.78		4.23	0.84		
Egf	3.81	1.69	6.39	1.00		2.67	0.89		
Egfr	1.07	0.17	1.47	0.33		1.48	0.17		
Ereg	1.11	0.28	6.24	1.09	<0.0001	9.84	0.86	<0.0001	ns
Fbn1	1.02	0.09	0.96	0.18		0.84	0.08		
Fgf2	1.05	0.15	0.97	0.22		0.72	0.09		
Foxp3	1.02	0.09	1.94	0.35		1.25	0.40		
Gapd	1.01	0.08	0.80	0.12		0.80	0.11		
Hsp70	1.00	0.04	1.06	0.07		1.00	0.08		
Ifng	2.92	1.31	5.09	4.66		2.65	1.03		

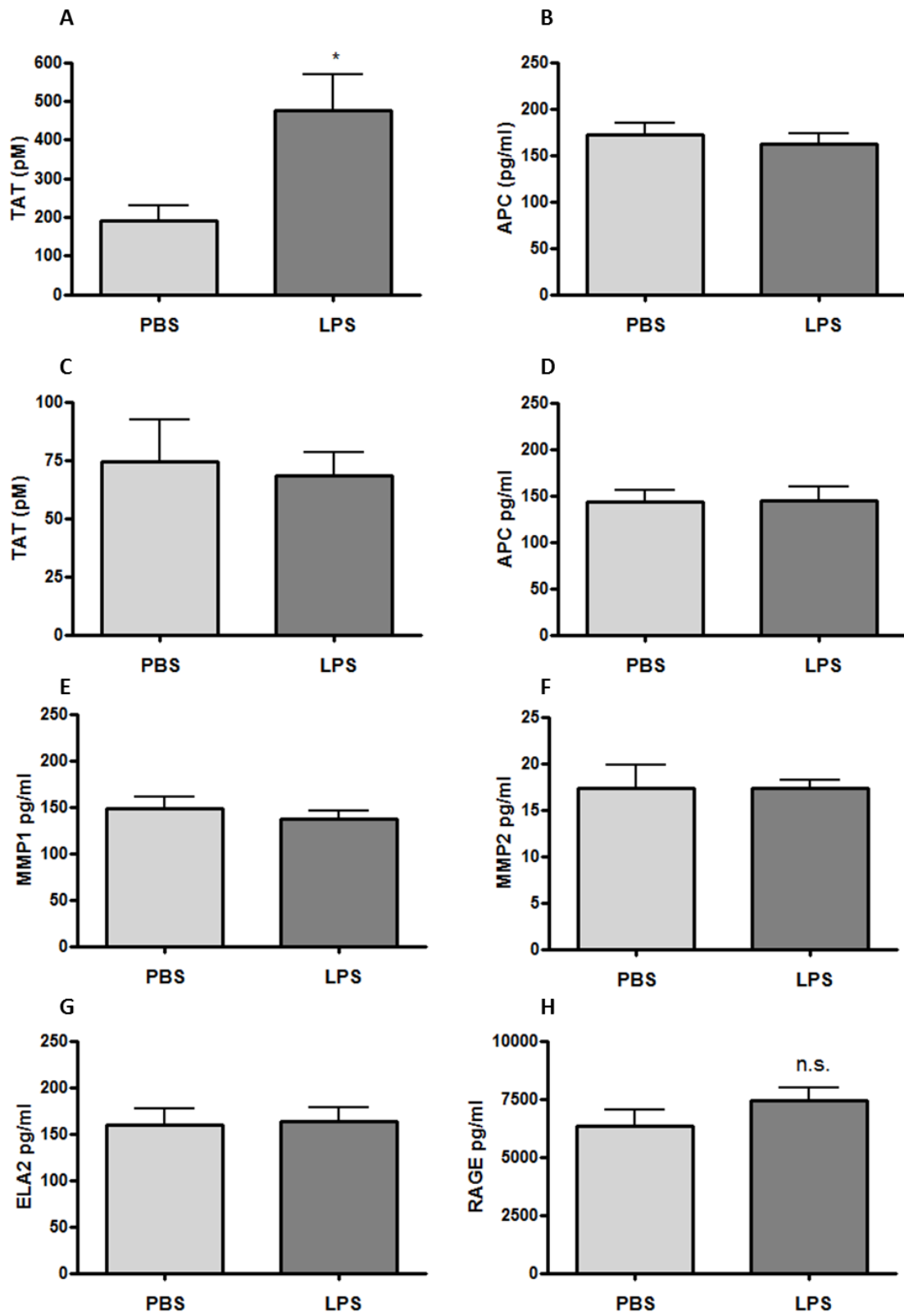
Il10	7.03	4.93	5.23	4.82		2.52	1.09		
Il10ra	1.02	0.11	2.33	0.39	<0.0001	1.39	0.12	ns	<0.05
Il10rb	1.01	0.06	1.61	0.19		1.44	0.14		
Il11	1.86	0.99	0.34	0.13		0.43	0.14		
Il12a	2.36	0.73	2.44	0.30		1.51	0.36		
Il12rb1	1.09	0.22	1.65	0.30		1.27	0.27		
Il12rb2	1.03	0.13	1.24	0.32		1.44	0.26		
Il13ra1	1.02	0.10	2.47	0.46		2.29	0.34		
Il13ra2	2.44	1.32	39.83	6.65	<0.0001	38.39	10.38	<0.0001	ns
Il16	1.01	0.06	0.96	0.08		0.93	0.10		
Il18	1.04	0.14	1.20	0.15		1.12	0.13		
Il1a	1.04	0.15	2.53	0.20	<0.0001	1.99	0.10	<0.0001	ns
Il1b	1.17	0.36	22.24	3.59	<0.0001	18.57	2.41	<0.0001	ns
Il1r1	1.03	0.13	1.55	0.22		1.71	0.21		
Il1r2	1.11	0.23	20.13	5.05	<0.0001	38.28	4.76	<0.0001	<0.05
Il2ra	1.23	0.37	2.21	0.40		2.26	0.14		ns
Il5	3.08	1.72	8.90	4.00		5.35	1.51		
Il6	1.09	0.22	27.82	6.28	<0.0001	28.18	2.68	<0.0001	ns
Il6ra	1.08	0.23	0.82	0.10		0.93	0.12		
Il7	1.04	0.13	0.65	0.08		0.55	0.09		
Mmp2	1.03	0.13	0.88	0.18		0.92	0.08		
Mmp3	1.05	0.16	1.74	0.27	<0.05	2.28	0.30	<0.01	ns
Mmp9	1.19	0.26	6.83	0.99	<0.0001	6.71	0.70	<0.0001	ns
Muc1	1.01	0.06	1.21	0.05		1.11	0.07		
Muc2	1.01	0.09	3.21	0.83		2.58	0.80		
Muc5b	1.05	0.15	0.99	0.23		0.96	0.11		
Pcoln3	1.04	0.13	1.31	0.16		1.36	0.15		
Pdgfb	1.01	0.05	0.93	0.05		0.69	0.04		
Pdgfb	1.01	0.09	1.08	0.12	ns	0.77	0.05	<0.05	<0.05
Pdgfc	1.05	0.16	0.75	0.04	ns	0.62	0.06	ns	<0.05
Pdgfd	1.01	0.06	1.13	0.14		1.03	0.13		
Pdgfrb	1.04	0.13	0.96	0.20		0.90	0.08		
Rab3b	1.10	0.26	0.78	0.18		0.98	0.24		
Retn	1.17	0.31	1.54	0.12		1.53	0.27		
Retnla	1.11	0.28	1.11	0.15		1.36	0.13		
Retnlg	1.07	0.18	11.32	1.47	<0.0001	22.73	2.57	<0.0001	<0.01
Serpinh1	1.02	0.10	1.09	0.14		0.61	0.08		
Sftpa	1.01	0.08	1.09	0.11		1.11	0.08		
Sftpb	1.01	0.09	0.78	0.05		0.89	0.06		
Sftpc	1.00	0.05	1.03	0.05		1.39	0.26		
Sftpd	1.02	0.10	2.17	0.20	<0.0001	2.43	0.23	<0.0001	ns
Tgfb1	1.01	0.05	1.24	0.19		0.97	0.07		

Tgfb1	1.01	0.07	1.35	0.29		1.06	0.12		
TGFbr1	1.05	0.18	0.92	0.13		0.74	0.09		
Tgfb2	1.02	0.10	0.91	0.22		0.73	0.08		
Tlr2	1.06	0.18	6.08	1.26	<0.0001	5.20	0.54	<0.0001	ns
Tlr3	1.05	0.15	2.37	0.47	<0.01	1.97	0.20	<0.05	ns
Tlr4	1.03	0.13	1.07	0.24		0.92	0.10		
Tlr9	1.02	0.09	1.64	0.32		1.07	0.12		
Tnc	1.01	0.07	1.17	0.23	ns	0.67	0.06	<0.05	<0.05
Tnf	1.10	0.25	14.34	2.44	<0.0001	14.15	0.94	<0.0001	ns
Txnrd1	1.06	0.19	1.94	0.39		1.84	0.25		
Vamp8	1.01	0.06	1.65	0.05		1.67	0.10		
Vegfa	1.03	0.12	0.80	0.12		0.65	0.07		
Vim	1.01	0.08	0.78	0.15		0.65	0.07		

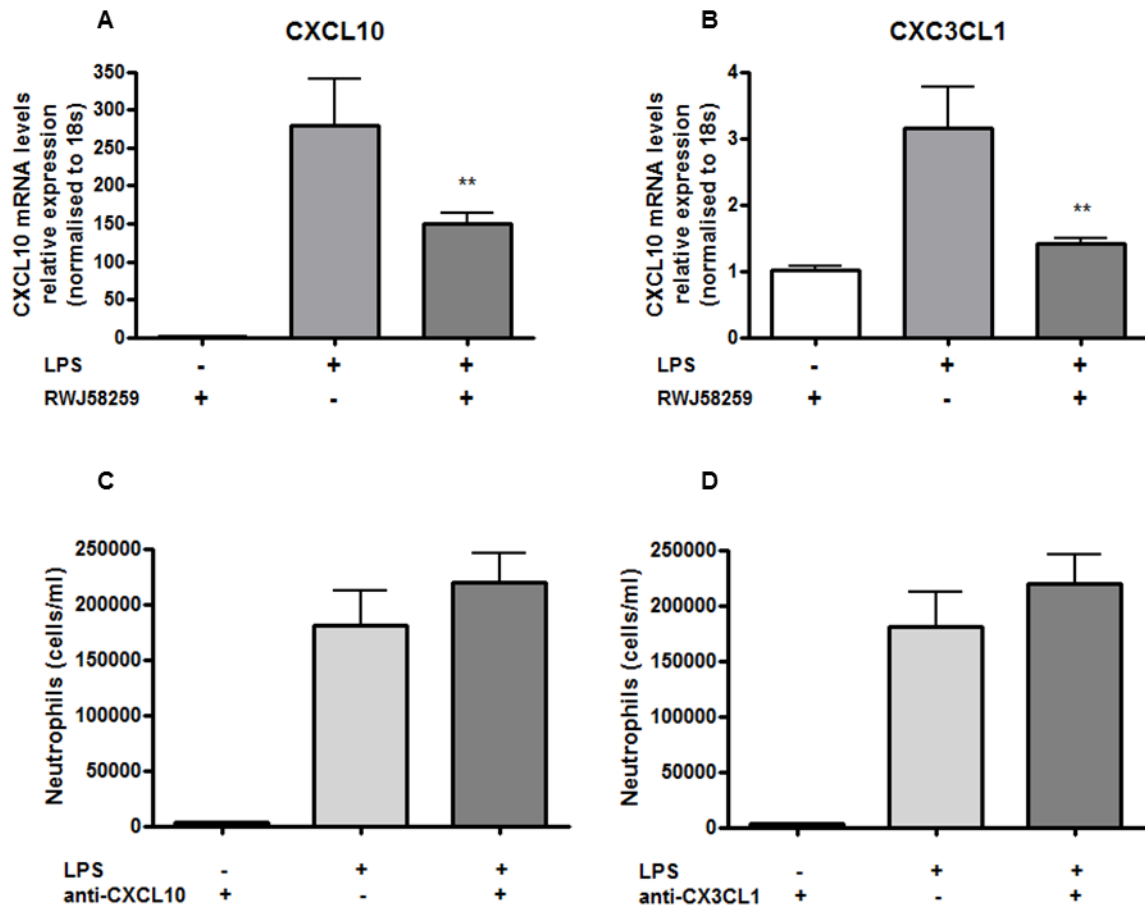
Supplementary Figure 1.



Supplementary Figure 2.



Supplementary Figure 3.



Supplementary Methods.

In vitro cell culture.

The bronchial epithelial cell line Beas2B or the macrophage cell line THP-1 were cultured in DMEM (Gibco) containing 10% fetal calf serum (Lonza), L-glutamine, penicillin and streptomycin (all Invitrogen). Prior to stimulation cells were washed twice with PBS and serum starved for 2 h in DMEM without 10% FCS. Cells were stimulated with 10 nM thrombin (Sigma), 100 ng/ml LPS (Sigma) or a combination of both. Alternatively, cells were stimulated with 20 ng/ml TNF (Invitrogen), 20 ng/ml IFN- γ (Invitrogen) or a combination of both. Supernatant was removed after 3 h and CCL2, CCL7 and IL-8 were measured by ELISA (Peprotech).

Supplementary Figure 4.

